0013-7227/07/$15.00/0
Printed in U.S.A.

Endocrinology 148(7):3419–3425

doi: 10.1210/en.2006-1541

Opposite Effects of Leptin on Bone Metabolism: A Dose-Dependent Balance Related to Energy Intake and Insulin-Like Growth Factor-I Pathway

Aline Martin, Valentin David, Luc Malaval, Marie-Hélène Lafage-Proust, Laurence Vico, and Thierry Thomas

Institut National de la Santé et de la Recherche Médicale, Unité 890, University Hospital, 42055 St-Etienne, France

Published data describing leptin effects on bone are at variance with both positive and negative consequences reported. These findings are consistent with a bimodal threshold response to serum leptin levels. To test this theory, two groups of female rats (tail-suspended and unsuspended) were treated with ip leptin at two different doses or vehicle for 14 d. In tail-suspended rats, low-dose leptin compensated the decrease in serum leptin levels observed with suspension and was able to prevent the induced bone loss at both the trabecular and cortical level (assessed by three-dimensional microtomography). In contrast, high-dose leptin inhibited femoral bone growth and reduced bone mass by decreasing bone formation rate and increasing bone resorption in both tail-suspended and unsuspended groups. High- and low-dose leptin administration resulted in a reduced medullar adipocytic volume in all groups. High-dose leptin (but not low) induced a decrease in body-weight abdominal fat mass and serum IGF-I levels. Thus, the observed bone changes at high-dose leptin are at least partly mediated by a leptin-induced energy imbalance. In conclusion, a balance between negative and positive leptin effects on bone is dependent on a bimodal threshold that is triggered by leptin serum concentration. Also, the negative effects of high leptin levels are likely induced by reduced energy intake and related hormonal changes. The respective part of each pathway will be unraveled by additional studies. (*Endocrinology* 148: 3419–3425, 2007)

LEPTIN, THE PRODUCT of the *obese* gene, is a circulating hormone involved in feeding behavior and energy homeostasis (1, 2). In addition to its role as a hormonal regulator of body weight, leptin directly alters most of the endocrine pathways at both the pituitary and peripheral gland levels (3). Leptin deficiency leads to a variety of phenotypic abnormalities as well as obesity. Specifically, leptin is a pleiotropic hormone involved in regulation of a large variety of physiological processes, including the protective effects exerted by fat mass on the skeleton (4).

However, published data describing leptin effects on bone remain conflicting, with both positive and negative effects reported. Ducy *et al.* (5) found that icv injections of leptin decreased bone mass in both *ob/ob* mice and lean rodents (6). In contrast, with animals and osteoblasts lacking clock genes (7) (control circadian physiological rhythms), the opposite occurs (increased bone mass). Other studies in *ob/ob* mice confirm a stimulatory effect of ip leptin administration on bone tissue, specifically, a dramatic increase in cortical bone formation and a reversal of defective bone growth and osteopenia that occur in untreated *ob/ob* mice (8). This happens despite a 40% decrease in food intake and a 14% decrease in body weight (9). We showed recently that low ip dose of leptin prevented disuse-induced bone loss in lean rats (10) and partially prevents ovariectomy-induced bone loss in rats (11). Two different pathways mediate leptin effects on bone. The first is a central and negative pathway through the hypothalamic nuclei and the β-adrenergic system. The second is a peripheral positive pathway targeted directly toward leptin-specific receptors expressed by cells of osteoblastic lineage (12). To resolve these seemingly contradictory results, we propose that both pathways are balanced by diverse factors, including energy intake and serum leptin levels (for review, see Ref. 13).

Although studies evaluating the effects of icv leptin administration imply a single central pathway, peripheral administration suggests both direct and indirect cascades because cerebrospinal fluid leptin levels depend on serum concentrations (14). Thus, the latter would represent a more "physiological" process. Therefore, we hypothesized that leptin effects on the skeleton are dependent on administered dose, which could partly explain some of the differences reported in the literature. Indeed, several *in vitro* studies do confirm dose-dependent results, but no *in vivo* study has examined the bone metabolism response to different leptin doses. Hence, we evaluated bone tissue changes in response to two different ip administered leptin doses in a rat model of disuse-induced osteoporosis. Also, we examined leptin action on bone regarding hormonal and energetic balance changes because bone metabolism depends on hormonal

First Published Online April 12, 2007

Abbreviations: BFR, Bone formation rate; BMD, bone mineral density; BS, bone surface; BV, bone volume; Conn.D., connectivity density; Ct.Ar., cortical area; CTX, C. telopeptide of collagen type I; 3D, three-dimensional; DA, degree of anisotropy; dLS, double-labeled mineralizing surface; DXA, dual-energy x-ray absorptiometry; I_{min}, area moment of inertia along the small axis; I_{max}, area moment of inertia along the large axis; leptin 50, 50 μg/kg·d dose of leptin; leptin 500, 500 μg/kg·d dose of leptin; MAR, mineral apposition rate; pMOI, polar moment of inertia; OC, osteocalcin; ROI, region of interest; SMI, structure model index; TV, total volume.

***Endocrinology* is published monthly by The Endocrine Society (http://www.endo-society.org), the foremost professional society serving the endocrine community.**

status and body weight, two parameters directly under the control of leptin (15).

Materials and Methods

Animals

This animal interventional study was in accordance with the Declaration of Helsinki principles and was approved by the authors' institutional review board (Ministère de l'Agriculture, Paris, France; authorization no. 04827). Seventy 11-wk-old female Wistar rats (Iffa Credo, L'Arbresle, France), 240 ± 10 g mean body weight, were acclimatized for 1 wk with standard conditions of temperature (23 ± 1 C) and light/dark (11-h light, 13-h dark). Animals were individually housed and provided with food (standard diet with UAR A03) and water *ad libitum*. The rats were randomly assigned in seven groups of 10 animals each, depending on whether they were tail-suspended or nonsuspended, and treated by murine recombinant leptin, kindly provided by Amgen (Neuilly-sur-Seine, France) or its vehicle, for 14 d. A control group was killed at baseline. The suspension procedure was performed according to the recommendations of Wronski and Morey-Holton (16). Leptin was continuously administered using ip osmotic pumps (Alzet; Charles River, L'Arbresle, France) at two different doses: 50 (leptin 50) and 500 (leptin 500) μg/kg·d, with the lowest dose selected for having no significant effects on body weight. Food intake and body weight were measured every day and on d 0, 3, 5, 7, 10, 12, and 14, respectively. Fluorochrome double bone labeling was performed 5 and 1 d before the animals were killed with 25 mg/kg tetracycline ip injections. The rats were killed by either cervical dislocations on five rats per group or overdose of ketamine-xylazine solution on the other five.

Serum measurement

Blood samples were collected in heparinized tubes for measurement of serum leptin, IGF-I, and C. teleoptide of collagen type I (CTX) levels. For leptin assay, the rat leptin ELISA kit (Linco Research, St. Charles, MO) was used. For IGF-I assay, the rat/mouse IGF-I OCTEIA kit (Immunodiagnostic Systems, Fountain Hills, AZ) was used. For CTX assay, the RatLaps ELISA immunoassay (Nordic Biosciences Diagnostics, Herlev, Denmark) was used, following recommendations of the manufacturers.

Dual-energy x-ray absorptiometry (DXA)

A dual-energy x-ray PIXImus densitometer (Lunar Corp., Madison, WI) with small animal software was used for measuring bone mineral density (BMD) on d 0, 7, and 14. Rats were anesthetized with ip administration of 0.1–0.3 mg/kg ketamine-xylazine solution over the duration of the procedure. After image acquisitions, three different sites were determined by readjusting the region of interest (ROI) on left hindlimb: tibial proximal metaphysis, femoral diaphysis, and total femur. The tibial metaphysis zone, a 5.04- × 5.22-mm fixed rectangle positioned over the longitudinal axis of the proximal tibia, corresponds to one of the most responsive bone site to unloading induced by the suspension. The femoral diaphysis zone, a 6.48- × 17.1-mm fixed rectangle positioned over the longitudinal axis of diaphysis, corresponds to a representative cortical bone site. For total femur, ROI was adjusted on each bone length. In addition, abdominal fat mass was evaluated in an ROI delineated by L1 and L5 vertebrae and including the whole body width.

Bone length measurement

Bone growth was assessed by measuring length of five right femurs per group with a slide caliper.

High-resolution microtomography

Left femora were scanned *ex vivo* with high-resolution microtomography (VivaCT40; Scanco Medical, Bassersdorf, Switzerland). Data were acquired at 10.5 μm isotropic voxel size, with 2000 projections, 250 msec integration time, 55 keV photon energy, and 109 μA intensity.

Bones were measured inside a hemolysis tube. Three-dimensional (3D) trabecular parameters were evaluated using a fixed Gaussian filter.

Cancellous bone analysis

For cancellous bone analyses, a region of 419 transverse slices (4.2 mm) on the distal femoral growth plate was acquired, and the net scanning time was about 25 min. Bone surface (BS) were calculated using a tetrahedron meshing technique generated by the "marching cubes method" (17), and total volume (TV) was taken as the volume of interest. The bone volume fraction (BV/TV) was calculated directly by plotting gray voxels representing bone fraction against gray plus black voxels (nonbone objects), and normalized indices (BV/TV, BS/TV, and BS/BV) were used.

3D metric indices were calculated using direct techniques based on the distance transformation (18), without assuming a constant model. Direct indices (*i.e.* trabecular thickness, trabecular separation, and trabecular number) were calculated following the distance transformation method (18, 19).

The plate-rod characteristic of the structure was estimated by the structure model index (SMI) (20). The geometric degree of anisotropy (DA) was defined as the ratio between the maximal and minimal radius of the mean intercept length ellipsoid (21, 22). Connectivity density (Conn.D.) was calculated using the Euler method of Odgaard and Gundersen (23).

Cortical analysis

To analyze the cortex, we scanned a cross-sectional region of 109 transverse slices (1.1 mm) in the middle of the femur. For each measurement point acquired at the same settings, trabecular site, cortical area (Ct.Ar.), cross-sectional or total area, marrow area, cortical thickness, cortical porosity, and linear attenuation were evaluated, with the same Gaussian filter on a 0.5-mm region (50 slices). Distribution of bone mass was assessed by area moment of inertia along the small (I_{min}) and the large (I_{max}) axis, which are related to bending stiffness. Polar moment of inertia (pMOI), related to torsion stiffness, was also evaluated on the same region.

Histomorphometry

After the animals were killed, the left tibiae were immediately excised, fixed, dehydrated in absolute acetone, and embedded in methylmetacrylate at low temperature. Longitudinal frontal slices were cut from the embedded bones with a microtome (Polycut-S; Leica, Deerfield, IL). According to conventional histomorphometry analysis, six nonserial sections, 8-μm-thick, were used for modified Goldner staining, and 12-μm-thick sections were used to determine the dynamic indices of bone formation [*i.e.* double-labeled mineralizing surface (dLS/BS), mineral apposition rate (MAR), and bone formation rate (BFR/BS)]. MAR was derived from fluorochrome interlabel distances. BFR/BS was subsequently obtained as the product of dLS/BS and MAR. Six-micrometer-thick sections were used for tartrate-resistant acid phosphatase staining, allowing determination of the osteoclastic parameters (*i.e.* active osteoclast surfaces/BS and osteoclast number/bone area). For each section, data were collected in 2.6-mm-height ROIs within the secondary spongiosa. BV and parameters reflecting trabecular structure were measured using an automatic image analysis system (Biocom, Lyon, France). Bone cellular and macroscopic parameters were measured with a semiautomatic device: a digitizing tablet (Summasketch; Summagraphics, Paris, France) connected to a microcomputer with software designed in our laboratory. In addition, adipocytic parameters (*i.e.* adipocyte volume/marrow volume, adipocyte number, and adipocyte area) were measured on Goldner staining sections using the same method as for bone cellular and macroscopic parameters.

Tissue protein assessment

Total proteins were extracted from five right femoral distal metaphysis per group, ground in 2 ml lysis buffer containing 10 ml/liter Nonidet P-40, 1.8 g/liter iodoacetamide, 3.5 ml/liter proteases inhibition cocktail (Sigma, St. Quentin Fallavier, France), and 2 μl β-mercaptoethanol. After centrifugation (5 min, 5000 rpm, 4 C), supernatant samples were stored at −20 C. Osteocalcin (OC) content was measured by RatMID Osteocalcin ELISA kit (Nordic Biosciences Diagnostics, Herlev, Denmark), following manufacturer recommendations, whereas total

protein content was quantified with the colorimetric BCA kit (Pierce-Uptima, Interchim, Montluçon, France).

Statistical analysis

The statistical analyses were performed using Statistica software (StatSoft, Tulsa, OK). For time-dependent measures, data were analyzed using two-way ANOVA for "between-groups" effects and repeated-measures ANOVA for "within-group" effects. For one-point measurements, one-way ANOVA was performed. When F values for a given variable were found to be significant, the *post hoc* Scheffé's test was subsequently used. Results were considered significantly different at $P < 0.05$.

Results

Food intake, body weight, and abdominal fat mass

As expected, body weight of nonsuspended rats under vehicle significantly increased after 2 wk compared with baseline values, whereas it did not significantly change in suspended rats under vehicle or leptin 50 and nonsuspended rats under leptin 50 (Fig. 1A). Concurrently, abdominal fat mass significantly decreased in the suspended group under vehicle (Fig. 1B) together with a 68% significant reduction in serum leptin levels compared with those of the nonsuspended group under vehicle after 2 wk. Administration of a low dose of leptin compensated this suspension-induced decrease in serum leptin. Of note, serum leptin levels of groups under vehicle and leptin 50 remained in a physiological range (Table 1).

In contrast, a high dose of leptin induced a significant increase in plasma leptin levels for both controls and suspended animals (Table 1). In response, food intake was significantly reduced in these leptin 500 rats after 2 wk, inducing a decrease in body weight through loss of fat mass (Fig. 1B). This reduction in energy intake was associated with a dramatic decrease in serum IGF-I levels in both suspended and nonsuspended groups under this high dose of leptin (Table 1).

Femoral BMD

We measured a 7.4% increase in total femur BMD of nonsuspended rats under vehicle at d 14 compared with d 0 measurement ($P < 0.01$), although it did not change in the suspended group under vehicle. A similar 9.9% increase occurred in nonsuspended animals under leptin 50 ($P < 0.01$), whereas no significant change were observed over 2 wk in the suspended group under leptin 50 as well as in both groups under leptin 500.

Femoral diaphysis BMD increased by 9.4% ($P < 0.05$) and 10.7% ($P < 0.01$) over the 14 d of experimentation in the nonsuspended groups under vehicle and leptin 50, respectively. Although suspension blocked this increase in the group under vehicle, femoral diaphysis BMD significantly increased by 3.2% in the suspended group under leptin 50 ($P < 0.05$). No gain in femoral diaphysis BMD was observed in both suspended and nonsuspended groups treated with a high dose of leptin (Fig. 2).

Femoral length (Fig. 3)

Femoral length of nonsuspended rats under vehicle significantly increased over 2 wk of experiment compared with baseline group values. In contrast, no significant difference in femoral length was observed between suspended and baseline group values. Administration of a low dose of leptin prevented suspension effects on bone growth. Conversely, when administered at a high dose, leptin inhibited bone growth because no significant differences in femoral bone length between baseline group and both leptin 500 group values were observed, regardless of suspension.

3D evaluation of cortical envelope at femoral midshaft (Table 2)

Cortical 3D parameters increased in the nonsuspended group under vehicle over the 14 d of experimentation. Cor-

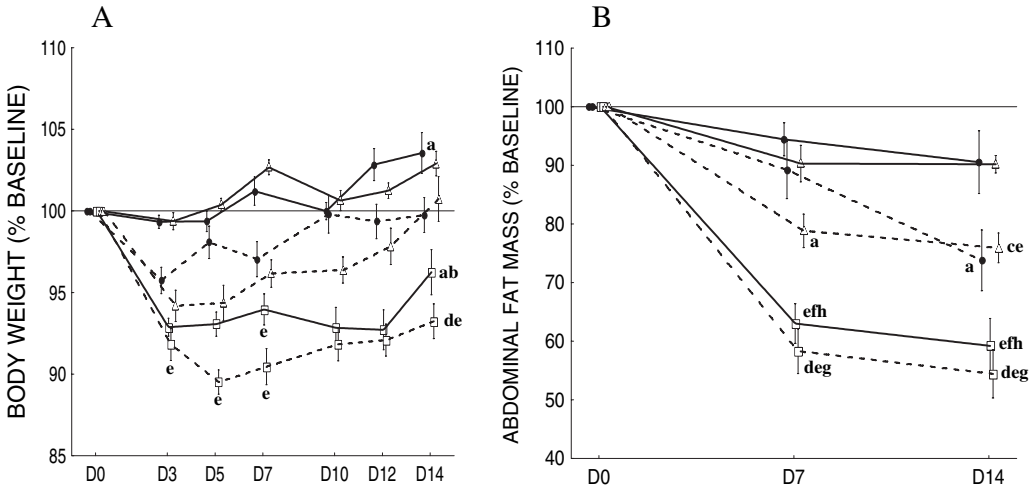

FIG. 1. Evolution of cumulative body weight (A) and abdominal fat mass (B) over a 2-wk period in tail-suspended (*dotted lines*) or nonsuspended (*solid lines*) female rats treated with 50 (*triangles*) or 500 (*squares*) μg/kg·d ip murine leptin or vehicle (*filled circles*). Values are mean ± SE of 10 female rats per group for body weight and eight female rats per group for abdominal fat mass. Comparisons were performed using two-way (between-groups effects) and repeated-measures (within-group effects) ANOVA and *post hoc* Scheffé's test. For reading convenience, significant differences are given only at d 3, 7, and/or 14. $P < 0.05$ *vs.* the following: [a] d 0; [b] nonsuspended vehicle; [c] nonsuspended leptin 50; [d] suspended leptin 50. $P < 0.01$ *vs.* the following: [e] d 0; [f] nonsuspended vehicle; [g] suspended vehicle; [h] nonsuspended leptin 50.

TABLE 1. Effects of leptin treatment on biochemical parameters

	Baseline	Vehicle		Leptin 50		Leptin 500	
		Nonsuspended	Suspended	Nonsuspended	Suspended	Nonsuspended	Suspended
Leptin (ng/ml)	1.5 ± 0.4	2.1 ± 0.9	0.7 ± 0.2^{a,g}	1.6 ± 0.8	4.2 ± 1.6^{a,c,d}	23.5 ± 15.8^{a,b,d}	29.0 ± 3.6^{a,b,c,d,e}
IGF-I (ng/ml)	1000.8 ± 144.1	1479.3 ± 147.3^{a}	1195.0 ± 130.3	1401.3 ± 204.3^{a}	1081.7 ± 176.7^{b}	759.2 ± 100.8^{g,h}	683.3 ± 54.1^{c,g,h}
CTX (ng/ml)	10.4 ± 0.2	12.3 ± 0.4	12.4 ± 1.2	13.0 ± 2.3	12.5 ± 0.3	16.4 ± 1.3^{f}	15.7 ± 2.2^{a}
OC (ng/μg of proteins)	0.55 ± 0.12	0.34 ± 0.04^{f}	0.18 ± 0.01^{b,f}	0.27 ± 0.02^{f}	0.23 ± 0.02^{f}	0.15 ± 0.01^{f,g}	0.14 ± 0.01^{f,g}

Animals were tail suspended or not and treated with two different doses of ip murine leptin (50 or 500 μg/kg·d) or vehicle for 14 d. A group of control rats was killed at baseline. Leptin, IGF-I, and CTX plasma values are mean ± SD of four female rats per group. OC and total proteins were extracted from five right femoral distal metaphysis per group. Comparisons were performed using one- and two-way (between-groups effects) ANOVA and *post hoc* Scheffé's test.

$P < 0.05$ *vs.* the following: [a] baseline; [b] nonsuspended vehicle; [c] suspended vehicle; [d] nonsuspended leptin 50; [e] suspended leptin 50. $P < 0.01$ *vs.* the following: [f] baseline; [g] nonsuspended vehicle; [h] nonsuspended leptin 50.

tical bone growth was inhibited by tail suspension, whereas a low dose of leptin prevented these suspension effects on cortical bone. This was related to an increase in cross-sectional area with higher I_{max} and pMOI values, whereas marrow area did not change. Conversely, no difference in femoral diaphysis Ct.Ar. was observed between both groups treated with a high dose of leptin and baseline group, and I_{min} was significantly lower in all animals under leptin 500 compared with nonsuspended animals under vehicle.

Two-dimensional and 3D evaluation of trabecular bone at femoral and tibial metaphysis (Table 2)

A nonsignificant increase in distal femoral metaphysis BV/TV was observed in the nonsuspended group under vehicle after 2 wk compared with the baseline group. This was associated with lower SMI and DA values. Suspension induced a trend in lower femoral metaphysis BV/TV with significantly higher SMI, whereas no difference was observed for both Conn.D. and DA parameters between suspended and nonsuspended groups. Suspension also induced a 6.5% loss in proximal tibia metaphysis BMD over time, as assessed by DXA (Fig. 4).

A low dose of leptin partially prevented this suspension-induced decrease in BMD, and microarchitectural parameters SMI and Conn.D. were significantly better in suspended rats under leptin 50 than in suspended rats under vehicle. Conversely, a high dose of leptin stimulated the suspension-induced loss in both distal femoral metaphysis BV/TV and proximal tibia metaphysis BMD (Fig. 4). No change in Conn.D. and SMI were observed in both groups under leptin 500.

Cellular and biochemical parameters

In accordance with previous reports (10, 24, 25), osteoclast activity was decreased after 2 wk in suspended rats under vehicle (osteoclast surface/BS of 1.0 ± 0.6 *vs.* 2.2 ± 1.1% at baseline; $P < 0.05$), and leptin did not alter bone resorption at

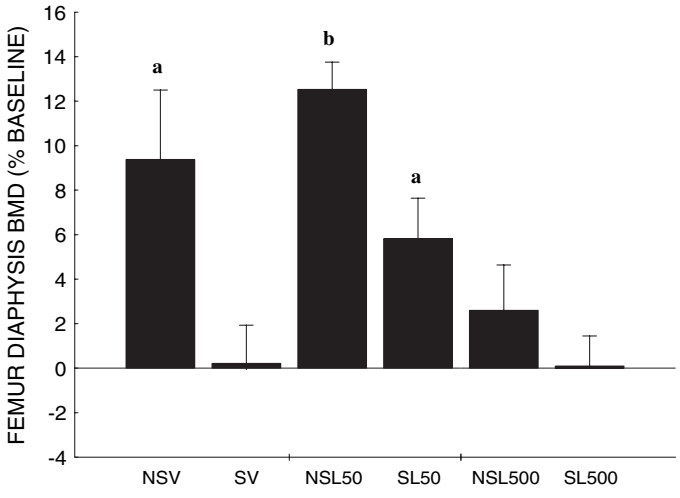

FIG. 2. Effect of ip leptin treatment at 50 or 500 μg/kg·d (L50 or L500) or vehicle (V) over 14 d in tail-suspended (S) or nonsuspended (NS) female rats, on femoral diaphysis BMD assessed by DXA. Values are mean ± SE, expressed as percentage of baseline, of eight female rats per group. Comparisons were performed using one- and two-way (between-groups effects) and repeated-measures (within-group effects) ANOVA and *post hoc* Scheffé's test. $P < 0.05$ *vs.* [a] d 0; $P < 0.01$ *vs.* [b] d 0.

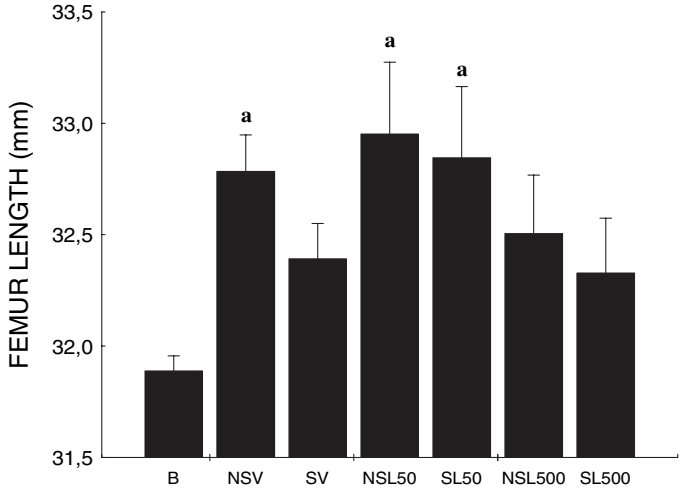

FIG. 3. Effect of ip leptin treatment at 50 or 500 μg/kg·d (L50 or L500) or vehicle (V) over 14 d in tail-suspended (S) or nonsuspended (NS) female rats, on femur length. A group of control rats was killed at baseline (B). Values are mean ± SE of five female rats per group. Comparisons were performed using one- and two-way (between-groups effects) ANOVA and *post hoc* Scheffé's test. $P < 0.01$ *vs.* [a] baseline.

TABLE 2. Effects of leptin treatment on femoral trabecular and cortical bone parameters assessed by 3D-microtomography

	Baseline	Vehicle		Leptin 50		Leptin 500	
		Nonsuspended	Suspended	Nonsuspended	Suspended	Nonsuspended	Suspended
Trabecular parameters							
VOX BV/TV (%)	29.9 ± 3.1	34.5 ± 1.6	30.0 ± 5.0	28.4 ± 3.4	30.2 ± 4.2	29.9 ± 5.2	28.0 ± 4.1
SMI	0.9 ± 0.3	0.7 ± 0.3	1.2 ± 0.1[g]	0.9 ± 0.1	0.7 ± 0.4[h]	0.8 ± 0.4	1.1 ± 0.3[b,e]
DA	1.8 ± 0.1	1.7 ± 0.1[f]	1.8 ± 0.1[f]	1.8 ± 0.1[f]	1.7 ± 0.1[f]	1.7 ± 0.1[f,g,i]	1.7 ± 0.1[b,c,f]
Conn.D. (mm^3)	152.9 ± 20.1	188.1 ± 10.6[a]	188.3 ± 26.6[a]	187.3 ± 42.4[a]	203.8 ± 19.2[f]	168.8 ± 34.6	167.3 ± 19.3[j]
Cortical parameters							
Ct.Ar. (mm^2)	4.6 ± 0.1	5.0 ± 0.2[f]	4.9 ± 0.1	5.0 ± 0.1[f]	5.0 ± 0.2[f]	4.9 ± 0.1	4.9 ± 0.1
Cr.Sc.Ar. (mm^2)	10.4 ± 0.5	11.3 ± 0.6	11.0 ± 0.6	11.5 ± 0.6[a]	11.2 ± 0.5	10.7 ± 0.3	11.6 ± 0.4[a]
Ma.Ar. (mm^2)	5.9 ± 0.5	6.3 ± 0.6	6.0 ± 0.6	6.6 ± 0.6	6.2 ± 0.3	5.9 ± 0.2	6.7 ± 0.3
I_{min}	3.0 ± 0.3	3.9 ± 0.4[f]	3.4 ± 0.3[a,g]	3.9 ± 0.3[b,f]	3.6 ± 0.2[b,f]	3.4 ± 0.4[a,g,i]	3.5 ± 0.4[a,b,d]
I_{max}	5.3 ± 0.5	5.8 ± 0.7[a]	5.8 ± 0.3[a]	6.3 ± 0.6[f]	6.1 ± 0.5[f]	5.6 ± 0.3[i]	5.7 ± 0.6[i]
pMOI	8.9 ± 0.7	9.6 ± 1.1	9.2 ± 0.5	10.0 ± 1.0[f]	9.3 ± 0.7	8.7 ± 0.6[b,i]	9.3 ± 0.9

Animals were tail suspended or not and treated with two different doses of ip murine leptin (50 or 500 μg/kg·d) or vehicle for 14 d. A group of control rats was killed at baseline. 3D cancellous and cortical bone parameters were measured by microtomography at femoral distal metaphysis and femoral midshaft, respectively. Values are mean ± SD of eight female rats per group. Comparisons were performed using one- and two-way (between-groups effects) ANOVA and *post hoc* Scheffé's test. VOX, Volume fraction; Cr.Sc.Ar., cross-sectional or total area; Ma.Ar., marrow area.

$P < 0.05$ *vs.* the following: [a] baseline; [b] nonsuspended vehicle; [c] suspended vehicle; [d] nonsuspended leptin 50; [e] suspended leptin 50. $P < 0.01$ *vs.* the following: [f] Baseline; [g] nonsuspended vehicle; [h] suspended vehicle; [i] nonsuspended leptin 50; [j] suspended leptin 50.

d 14 (0.9 ± 0.3 and 1.2 ± 0.4% in suspended and nonsuspended groups under leptin 50 and 1.1 ± 0.1 and 1.4 ± 0.2% in suspended and nonsuspended groups under leptin 500, respectively).

Conversely, tail suspension induced a significant decrease in BFR in the suspended group compared with the nonsuspended group under vehicle, mainly related to a dLS/BS reduction. A low dose of leptin prevented these suspension-induced effects. In contrast, administration of a high dose of leptin further decreased BFR. Surprisingly, this was mainly related to a decrease in MAR rather than decrease in dLS/BS (Table 3).

As expected, tail suspension induced an increase in medullar adipocytic volume, whereas both low and high doses of leptin prevented this increase (Table 3).

Biochemical measurements at d 14 confirmed histomorphometric changes in bone formation, because OC level decreased in the right distal femoral metaphysis in the suspended group compared with the nonsuspended group under vehicle, and this decrease was prevented by leptin administration at a low dose. Conversely, no difference in serum CTX was measured between a low dose of leptin and vehicle-treated groups regardless of suspension, whereas leptin 500-induced increase in bone resorption was associated with elevated serum CTX level after 2 wk in both the nonsuspended and suspended groups compared with baseline group values (Table 1).

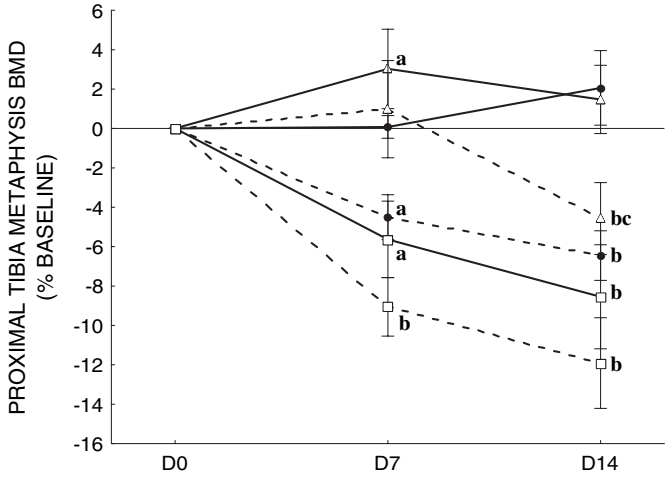

FIG. 4. Effect of ip leptin treatment at 50 or 500 μg/kg·d (L50 or L500) or vehicle (V) over 14 d in tail-suspended (S) or nonsuspended (NS) female rats, on proximal tibia metaphysis BMD measured by DXA. Values are mean ± SE, expressed as percentage of baseline, of eight female rats per group. Comparisons were performed using one- and two-way (between-groups effects) and repeated-measures (within-group effects) ANOVA and *post hoc* Scheffé's test. $P < 0.05$ *vs.* [a] d 0; $P < 0.01$ *vs.* [b] d 0 and [c] d 7.

Discussion

Considering the central role of leptin in driving hormonal and metabolic changes in response to energetic status, we postulated that its effects on bone result from direct and indirect pathways. These pathways are likely interdependent and regulated by the equilibrium between food intake and energy expenditure. This study is the first to address this postulate via an *in vivo* dose-response evaluation of leptin effects in a model of rapid bone loss.

On one hand, we demonstrated that low-dose (50 μg/kg·d) ip leptin treatment prevented suspension-induced BMD loss not only at a trabecular bone site (*i.e.* proximal tibial metaphysis) (10) but also at a cortical bone site (*i.e.* femoral diaphysis). High-resolution microtomography allowed us for the first time to analyze in more details those changes in both trabecular and cortical envelopes. Although mechanical unloading induced a rod-like trabecular structure (26), we showed that leptin treatment at physiological concentrations was able to preserve a plate-like cancellous pattern with better trabecular connectivity in suspended animals. In addition, it prevented tail suspension-induced cortical bone changes, including Ct.Ar. and minimal cross-sectional moment of inertia (I_{min}), two parameters related to mechanical strength of bone. This agrees with previous studies showing that ip leptin administration increased cortical bone mass in *ob/ob* mice (9) and reduced bone fragility by increased work to fracture in adult male mice (27). This is also consistent with the recent quantitative microtomography

TABLE 3. Effects of leptin treatment on bone formation parameters and medullar adipocytic volume measured by histomorphometry at secondary spongiosa of proximal tibial metaphysis level

	Baseline	Vehicle		Leptin 50		Leptin 500	
		Nonsuspended	Suspended	Nonsuspended	Suspended	Nonsuspended	Suspended
Bone formation parameters							
dLS/BS (%)	2.8 ± 1.0	4.1 ± 0.7	1.4 ± 0.3[f]	4.3 ± 1.2	2.1 ± 0.4[f,h]	3.3 ± 1.3	0.9 ± 0.2[a,f,h,i]
MAR (μm/d)	1.6 ± 0.1	1.8 ± 0.2	1.7 ± 0.1	1.5 ± 0.1	1.3 ± 0.1[a,f,g]	1.5 ± 0.2[b]	1.3 ± 0.3[f,g,i]
BFR/BS ($\mu m^2/\mu m^3$·d)	4.5 ± 1.4	7.5 ± 1.7	2.6 ± 0.9[d]	6.6 ± 2.3	4.2 ± 2.6[g]	3.9 ± 2.2[f]	1.1 ± 0.3[a,d,f,h]
Medullar adipocyte parameters							
Ad.V/MV (%)	0.9 ± 0.3	0.5 ± 0.2[e]	1.0 ± 0.7[f]	0.7 ± 0.2	0.6 ± 0.2[c]	0.4 ± 0.1[e]	0.3 ± 0.2[e,g]

Animals were tail suspended or not and treated with two different doses of ip murine leptin (50 or 500 μg/kg·d) or vehicle for 14 d. A group of control rats was killed at baseline. Values are mean ± SD of eight female rats per group. Comparisons were performed using one- and two-way (between-groups effects) ANOVA and *post hoc* Scheffé's test. Ad.V/MV, Adipocyte volume/marrow volume.

$P < 0.05$ *vs.* the following: [a] baseline; [b] nonsuspended vehicle; [c] suspended vehicle; [d] suspended leptin 50. $P < 0.01$ *vs.* the following: [e] baseline; [f] nonsuspended vehicle; [g] suspended vehicle; [h] nonsuspended leptin 50; [i] nonsuspended leptin 500.

demonstration that *ob/ob* mice had reduced femoral cortical mass and density (28).

In addition, low-dose leptin administration counteracted the negative effects of unloading on bone growth (29, 30) by increasing both femoral-length and femoral-midshaft cortical area despite suspension. These data support the notion that leptin acts as a bone growth factor but do not resolve whether the effects are directly or indirectly mediated by the IGF pathway (31–33). Because in our study, serum IGF-I levels remained unchanged in all "low-dose" leptin groups, we conclude that leptin can stimulate bone growth independently of peripheral IGF-I.

Interestingly, a rodent model of growth inhibition by caloric restriction also showed similar changes (34). However, *in vitro* studies showed that these effects might combine direct stimulatory effects of leptin on chondrocytes and indirect effects mediated by increased IGF receptor expression (31, 34). Also, a similar study that used dichorionic twins showed that leptin levels relate to bone parameters only when the IGF axis remains unaltered (35).

Conversely, high-dose (500 μg/kg·d) ip leptin treatment completely inhibited BMD gain at different femoral sites in all conditions and even further decreased suspension-induced bone loss in proximal tibia metaphysis. Also, our data showed the negative effects of high-dose leptin on bone microarchitecture, including lower trabecular connectivity and a more rod-like organization of trabecular network (as measured by a lower DA and higher SMI). High-dose leptin also inhibited femoral bone growth in length, cortical expansion, and consequently cortical moments of inertia, regardless of suspension condition. Interestingly, these data are in line with those of Maor *et al.* (31), which also showed dual effects of leptin on chondrocyte proliferation with inhibitory effect at high dose.

Based on these observations of dual leptin dose-dependent effects on bone phenotype, we further questioned whether this was because of differences in bone formation response. We confirmed previously published results using different models (10, 11, 27), because a low dose of leptin was able to prevent the disuse-induced decrease in BFR with significantly higher mineralizing surfaces, reflecting active osteoblast number. These effects could be because of leptin mitogenic (34, 36, 37) and antiapoptotic effects (38) on osteoblast lineage.

In marked contrast to the low-dose leptin groups, high-dose administration increased the disused-induced reduction in BFR. This was partly related to a lowered MAR. Because similar patterns of bone formation changes are seen with icv administration of leptin (5), we believe that a predominant control occurs through a hypothalamic relay (5) when serum leptin exceeds a threshold value. Furthermore, administration of a high dose of leptin concurrently stimulated bone resorption, as measured by serum CTX levels (increased in both suspended and nonsuspended groups). This is also consistent with the central control of leptin on bone resorption, which is mediated by a combination of both sympathetic nervous system and CART (cocaine amphetamine-regulated transcript) effects (39). In these circumstances, it could even surpass unloading-induced bone loss, which is also partly mediated by the sympathetic system (40).

However, other indirect mechanisms are also likely involved. The reciprocal differentiation of osteoblasts and adipocytes (41), which is modulated by numerous growth factors including leptin (10, 42), is one possible mechanism. Of note, we observed an even higher decrease in medullar adipocyte volume under high-dose leptin. This was regardless of suspension, in agreement with the negative feedback mediated by leptin on adipocyte differentiation (43).

Because high-dose leptin induced loss of weight and abdominal fat mass in both suspended and nonsuspended rats, it could alter numerous hormonal pathways linked to weight changes (15). In fact, we noted in both suspended and nonsuspended groups a dramatic decrease in serum IGF levels. Also, these changes did not occur in nonsuspended groups treated with either vehicle or a low dose of leptin. This suggests that the low levels of IGF-I are attributable to a combination of direct leptin and starvation-induced effects (34).

In conclusion, we found a bimodal effect of leptin on bone growth and bone remodeling. A positive outcome occurs in tail-suspended rats administered leptin below a defined threshold level. This is likely because of a compensation of the decreased leptin levels caused by the tail suspension. In contrast, supraphysiological administration of leptin that exceeds a threshold level results in negative effects on bone regardless of the suspension condition. Clearly, central effects mediated by the sympathetic nervous system as well as hormonal changes related to decreased energy intake, body weight

loss, and inhibition of the IGF-I pathway play major roles. Additional studies will unravel the respective part of each pathway.

Acknowledgments

We thank Norbert Laroche for great technical assistance and Dr. Peter Rowe for thoughtful suggestions and editing review.

Received November 17, 2006. Accepted April 2, 2007.

Address all correspondence and requests for reprints to: Prof. Thierry Thomas, Institut National de la Santé et de la Recherche Médicale Unité 890, University Hospital, Boulevard Pasteur, 42055 St-Etienne Cedex 2, France. E-mail: thierry.thomas@univ-st-etienne.fr.

Disclosure Summary: The authors have nothing to disclose.

References

1. **Zhang Y, Proenca R, Maffei M, Barone M, Leopold L, Friedman JM** 1994 Positional cloning of the mouse obese gene and its human homologue. Nature 372:425–432
2. **Bray GA, York DA** 1979 Hypothalamic and genetic obesity in experimental animals: an autonomic and endocrine hypothesis. Physiol Rev 59:719–809
3. **Henry BA, Goding JW, Alexander WS, Tilbrook AJ, Canny BJ, Dunshea F, Rao A, Mansell A, Clarke IJ** 1999 Central administration of leptin to ovariectomized ewes inhibits food intake without affecting the secretion of hormones from the pituitary gland: evidence for a dissociation of effects on appetite and neuroendocrine function. Endocrinology 140:1175–1182
4. **Thomas T, Burguera B** 2002 Is leptin the link between fat and bone mass? J Bone Miner Res 17:1563–1569
5. **Ducy P, Amling M, Takeda S, Priemel M, Schilling AF, Beil FT, Shen J, Vinson C, Rueger JM, Karsenty G** 2000 Leptin inhibits bone formation through a hypothalamic relay: a central control of bone mass. Cell 100:197–207
6. **Elefteriou F, Takeda S, Ebihara K, Magre J, Patano N, Kim CA, Ogawa Y, Liu X, Ware SM, Craigen WJ, Robert JJ, Vinson C, Nakao K, Capeau J, Karsenty G** 2004 Serum leptin level is a regulator of bone mass. Proc Natl Acad Sci USA 101:3258–3263
7. **Fu L, Patel MS, Bradley A, Wagner EF, Karsenty G** 2005 The molecular clock mediates leptin-regulated bone formation. Cell 122:803–815
8. **Liu C, Grossman A, Bain S, Strachan M, Puerner D, Bailey C, Humes J, Lenox J, Yamamoto G, Sprugel K** 1997 Leptin stimulates cortical bone formation in obese (ob/ob) mice. J Bone Miner Res 12(Suppl 1):S115
9. **Steppan CM, Crawford DT, Chidsey-Frink KL, Ke H, Swick AG** 2000 Leptin is a potent stimulator of bone growth in ob/ob mice. Regul Pept 92:73–78
10. **Martin A, de Vittoris R, David V, Moraes R, Begeot M, Lafage-Proust MH, Alexandre C, Vico L, Thomas T** 2005 Leptin modulates both resorption and formation while preventing disuse-induced bone loss in tail-suspended female rats. Endocrinology 146:3652–3659
11. **Burguera B, Hofbauer LC, Thomas T, Gori F, Evans GL, Khosla S, Riggs BL, Turner RT** 2001 Leptin reduces ovariectomy-induced bone loss in rats. Endocrinology 142:3546–3553
12. **Thomas T, Gori F, Khosla S, Jensen MD, Burguera B, Riggs BL** 1999 Leptin acts on human marrow stromal cells to enhance differentiation to osteoblasts and to inhibit differentiation to adipocytes. Endocrinology 140:1630–1638
13. **Thomas T** 2004 The complex effects of leptin on bone metabolism through multiple pathways. Curr Opin Pharmacol 4:295–300
14. **Burguera B, Couce ME, Curran GL, Jensen MD, Lloyd RV, Cleary MP, Poduslo JF** 2000 Obesity is associated with a decreased leptin transport across the blood-brain barrier in rats. Diabetes 49:1219–1223
15. **Spiegelman BM, Flier JS** 2001 Obesity and the regulation of energy balance. Cell 104:531–543
16. **Wronski TJ, Morey-Holton ER** 1987 Skeletal response to simulated weightlessness: a comparison of suspension techniques. Aviat Space Environ Med 58:63–68
17. **Lorensen WE, Cline HE** 1987 Marching cubes: a high resolution 3D surface construction algorithm. Computer Graphics 21:163–169
18. **Hildebrand T, Ruegsegger P** 1997 A new method for the model independent assessment of thickness in three-dimensional images. J Microsc 185:67–75
19. **Hildebrand T, Laib A, Muller R, Dequeker J, Ruegsegger P** 1999 Direct three-dimensional morphometric analysis of human cancellous bone: microstructural data from spine, femur, iliac crest, and calcaneus. J Bone Miner Res 14:1167–1174
20. **Hildebrand T, Ruegsegger P** 1997 Quantification of bone microarchitecture with the structure model index. Comput Methods Biomech Biomed Engin 1:15–23
21. **Harrigan TP, Mann RW** 1984 Characterization of microstructural anisotropy in orthoptic materials using a second rank tensor. J Mater Sci 19:761–767
22. **Whitehouse WJ** 1974 The quantitative morphology of anisotropic trabecular bone. J Microsc 101:153–168
23. **Odgaard A, Gundersen HJ** 1993 Quantification of connectivity in cancellous bone, with special emphasis on 3-D reconstructions. Bone 14:173–182
24. **Vico L, Bourrin S, Very JM, Radziszowska M, Collet P, Alexandre C** 1995 Bone changes in 6-mo-old rats after head-down suspension and a reambulation period. J Appl Physiol 79:1426–1433
25. **Barou O, Valentin D, Vico L, Tirode C, Barbier A, Alexandre C, Lafage-Proust MH** 2002 High-resolution three-dimensional micro-computed tomography detects bone loss and changes in trabecular architecture early: comparison with DEXA and bone histomorphometry in a rat model of disuse osteoporosis. Invest Radiol 37:40–46
26. **David V, Laroche N, Boudignon B, Lafage-Proust MH, Alexandre C, Ruegsegger P, Vico L** 2003 Noninvasive in vivo monitoring of bone architecture alterations in hindlimb-unloaded female rats using novel three-dimensional microcomputed tomography. J Bone Miner Res 18:1622–1631
27. **Cornish J, Callon KE, Bava U, Lin C, Naot D, Hill BL, Grey AB, Broom N, Myers DE, Nicholson GC, Reid IR** 2002 Leptin directly regulates bone cell function in vitro and reduces bone fragility in vivo. J Endocrinol 175:405–415
28. **Baldock PA, Allison S, McDonald MM, Sainsbury A, Enriquez RF, Little DG, Eisman JA, Gardiner EM, Herzog H** 2006 Hypothalamic regulation of cortical bone mass: opposing activity of Y2 receptor and leptin pathways. J Bone Miner Res 21:1600–1607
29. **Dehority W, Halloran BP, Bikle DD, Curren T, Kostenuik PJ, Wronski TJ, Shen Y, Rabkin B, Bouraoui A, Morey-Holton E** 1999 Bone and hormonal changes induced by skeletal unloading in the mature male rat. Am J Physiol 276:E62–E69
30. **Sibonga JD, Zhang M, Evans GL, Westerlind KC, Cavolina JM, Morey-Holton E, Turner RT** 2000 Effects of spaceflight and simulated weightlessness on longitudinal bone growth. Bone 27:535–540
31. **Maor G, Rochwerger M, Segev Y, Phillip M** 2002 Leptin acts as a growth factor on the chondrocytes of skeletal growth centers. J Bone Miner Res 17:1034–1043
32. **Kume K, Satomura K, Nishisho S, Kitaoka E, Yamanouchi K, Tobiume S, Nagayama M** 2002 Potential role of leptin in endochondral ossification. J Histochem Cytochem 50:159–169
33. **Kishida Y, Hirao M, Tamai N, Nampei A, Fujimoto T, Nakase T, Shimizu N, Yoshikawa H, Myoui A** 2005 Leptin regulates chondrocyte differentiation and matrix maturation during endochondral ossification. Bone 37:607–621
34. **Gat-Yablonski G, Ben-Ari T, Shtaif B, Potievsky O, Moran O, Eshet R, Maor G, Segev Y, Phillip M** 2004 Leptin reverses the inhibitory effect of caloric restriction on longitudinal growth. Endocrinology 145:343–350
35. **Bajoria R, Sooranna SR, Chatterjee R** 2006 Type 1 collagen marker of bone turnover, IGF and leptin in dichorionic twins with discordant birth weight. J Clin Endocrinol Metab 91:4696–4701
36. **Takahashi Y, Okimura Y, Mizuno I, Iida K, Takahashi T, Kaji H, Abe HKC** 1997 Leptin induces mitogen-activated protein kinase-dependent proliferation of C3H10T1/2 cells. J Biol Chem 272:12897–12900
37. **Burguera B, Brunetto A, Garcia-Ocana A, Teijeiro R, Esplen J, Thomas T, Couce ME, Zhao A** 2006 Leptin increases proliferation of human osteosarcoma cells through activation of PI(3)-K and MAPK pathways. Med Sci Monit 12: BR341–BR349
38. **Gordeladze JO, Drevon CA, Syversen U, Reseland JE** 2002 Leptin stimulates human osteoblastic cell proliferation, de novo collagen synthesis, and mineralization: Impact on differentiation markers, apoptosis, and osteoclastic signaling. J Cell Biochem 85:825–836
39. **Elefteriou F, Ahn JD, Takeda S, Starbuck M, Yang X, Liu X, Kondo H, Richards WG, Bannon TW, Noda M, Clement K, Vaisse C, Karsenty G** 2005 Leptin regulation of bone resorption by the sympathetic nervous system and CART. Nature 434:514–520
40. **Kondo H, Nifuji A, Takeda S, Ezura Y, Ritling SR, Denhardt DT, Nakashima K, Karsenty G, Noda M** 2005 Unloading induces osteoblastic cell suppression and osteoclastic cell activation to lead to bone via sympathetic nervous system. J Biol Chem 280:30192–30200
41. **Meunier P, Aaron J, Edouard C, Vignon G** 1971 Osteoporosis and the replacement of cell populations of the marrow by adipose tissue. A quantitative study of 84 iliac bone biopsies. Clin Orthop Relat Res 80:147–154
42. **Ahdjoudj S, Lasmoles F, Holy X, Zerath E, Marie PJ** 2002 Transforming growth factor β2 inhibits adipocyte differentiation induced by skeletal unloading in rat bone marrow stroma. J Bone Miner Res 17:668–677
43. **Wagoner B, Hausman DB, Harris RB** 2006 Direct and indirect effects of leptin on preadipocyte proliferation and differentiation. Am J Physiol Regul Integr Comp Physiol 290:R1557–R1564